

Influence of Sintering Temperature on Densification, Structure and Microstructure of Li and Sb Co-Modified (K_{0.5}Na_{0.5})_{1-x}(Li)_x(Sb)_x(Nb)_{1-x}O₃-Based Ceramics

Rashmi Rani*, Seema Sharma

Ferroelectrics Research Laboratory, Department of Physics, A N College, Patna, India.

Email: *newton_rashmi51@yahoo.com

Received July 21st, 2011; revised September 20th, 2011; accepted September 29th, 2011.

ABSTRACT

Polycrystalline samples of Lead free ($K_{0.5}Na_{0.5}$)_{1-x}(Li)_x(Sb)_x(Nb)_{1-x}O₃ ceramics with nominal compositions ($x = 0.040$ to 0.060) have been prepared by high temperature solid state reaction technique. X-ray diffraction (XRD) pattern shows that the crystal structure transforms from orthorhombic to tetragonal as Li and Sb content increases. Normal sintering process yield compounds with density ~98.2% of the theoretical value. Densification of the Li and Sb co-doped KNN ceramics might be explained by the liquid-phase sintering. This may be attributed to the low melting temperature of Li compounds that appears to promote the formation of a liquid phase during sintering.

Keywords: KNN, Perovskite, XRD, SEM

1. Introduction

The speedy development of piezoelectric devices urgently calls for environment-friendly materials substituting for the widely used lead zirconate titanate (Pb Zr, Ti)O₃, (PZT)). Among various lead-free piezoelectric materials, ceramics based on potassium sodium niobate (KNbO₃-NaNbO₃) are most promising [1-5]. Highly dense (Na_{0.5}K_{0.5}) NbO₃ (KNN) ceramics was fabricated using hot pressing which possessed high piezoelectric constants [2]. It was even reported that KNN based ceramics were sensitive to moisture and only hot-pressed samples could be sufficiently densified [1,2]. Recently developed spark plasma sintering is another sintering method to produce dense bulk samples of KNN ceramics with a relative density higher than 99% [6,7]. Although pressure-assisted sintering processes are effective in consolidating KNN ceramics by lowering the sintering temperature and hence suppressing the volatilization of alkali components, it is obvious that normal or pressureless sintering of these materials is more suitable for mass production. Most recent studies have concentrated on the development of KNN-based lead-free ceramics with enhanced piezoelectric properties through doping or texture control [8-10].

On the basis of the reported work and the analogy of

PZT-based ceramics, it is noted that the key approach for improving the piezoelectric properties of KNN-based ceramics is to lower the ferroelectric tetragonal-ferroelectric orthorhombic phase transition (T_{O-F}), forming coexistence of the tetragonal and orthorhombic phases at room temperature. This could be achieved by partial substitutions of A-site ions (Na_{0.5}K_{0.5})⁺ and B-site ion (Nb)⁵⁺ by other analogous ions in the ABO₃-type (KNN) perovskite structure. In the present work, KNN ceramics partially substituted with Li⁺ and Sb⁺ were prepared by ordinary solid-state sintering, and their structure and microstructure properties were studied.

2. Experimental Section

2.1. Experimental Procedure

(K_{0.5}Na_{0.5})_{1-x}(Li)_x(Sb)_x(Nb)_{1-x}O₃ ceramics with nominal compositions ($x = 0.040, 0.045, 0.050, 0.055$ and 0.060) were prepared by conventional ceramic technique using analytical grades metal oxides or carbonate powders: K₂CO₃ (99%), Na₂CO₃ (99.8%), Li₂CO₃ (99.9%), Sb₂O₃ (99.9%), and Nb₂O₅ (99.5%). These powders were used as starting raw materials. For each composition, the starting materials were weighed according to the stoichiometric formula and ball-milled in acetone using zirconia balls for 24 h. After drying, the calcination was

carried out at 900°C, 890°C and 870°C for 4 h. The calcined powders were then pressed into 10mm diameter disks at 300 MPa. The disks samples were finally sintered between 1060°C - 1120°C for 4 h - 2 h in air. Silver electrodes were applied on the top and bottom surfaces of the samples for the measurements.

2.2. Sample Characterization

The formation and quality of compounds were verified with x-ray diffraction (XRD) technique. The XRD patterns of the compounds were recorded at room temperature using x-ray powder diffractometer (Rigaku Miniflex, Japan) with CuK α radiation ($\lambda = 1.5405 \text{ \AA}$) in a wide range of Bragg angles 2θ ($20^\circ \leq 2\theta \leq 60^\circ$) at a scanning rate of 2° min^{-1} . The microstructures were observed using a scanning electron microscope (SEM). These micrographs were obtained with a JEM-2000FX (JEOL Ltd.) scanning electron microscope operated at 20 KeV. Density of samples was determined using the Archimedes' method. The differential thermal analysis (DSC-TG), Setaram Labsys, Setaram Instrumentation, Caluire, France) of ceramics powders was carried out in air from room temperature to 800°C with different heating rates of 2° min^{-1} .

3. Results and Discussion

3.1. XRD Analysis

Figure 1 shows the room temperature XRD patterns of the $(1-x)\text{K}_{0.5}\text{Na}_{0.5}\text{NbO}_{3-x}\text{LiSbO}_3$ ceramics with $0.04 < x < 0.06$. It can be seen that a perovskite structure with a small amount of secondary phase $\text{K}_3\text{Li}_2\text{Nb}_5\text{O}_{15}$ with the

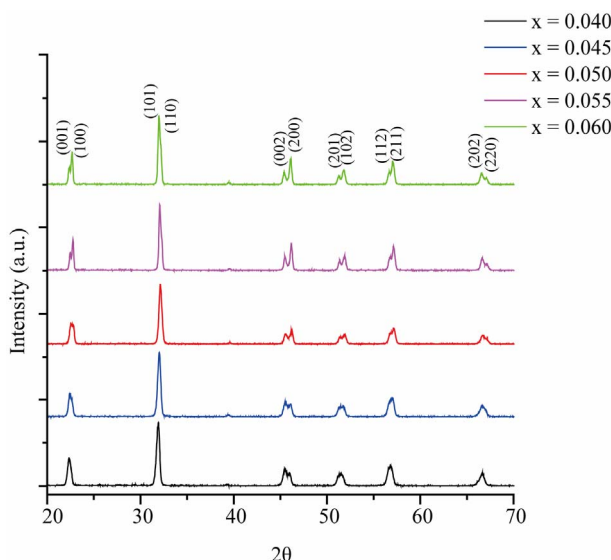


Figure 1. Room temperature XRD pattern of $(1-x)\text{K}_{0.5}\text{Na}_{0.5}\text{NbO}_{3-x}\text{LiSbO}_3$ ceramics.

tetragonal tungsten bronze structure is formed. The crystal structure changes from orthorhombic to tetragonal with increase in x . As the crystal structure of KNN (perovskite structure) is very different from LiSbO₃ (ilmenite structure), our results suggest that Li⁺ and Sb⁵⁺ have diffused into the KNN lattices, with Li⁺ entering the $(\text{Na}_{0.5}\text{K}_{0.5})^+$ sites and Sb⁵⁺ occupying the Nb⁵⁺ sites, to form a homogeneous solid solution. **Figure 2** shows the enlarged XRD patterns of the ceramics in the ranges of 2θ from 44° to 48° , respectively. It can be seen that at $x < 0.05$, the ceramic has an orthorhombic perovskite structure (the corresponding XRD patterns can be indexed by Ref [11]).

As x (i.e., the concentration of LiSbO₃) increases, a tetragonal phase appears and increases continuously. At $x > 0.05$, the ceramic begin to possess a tetragonal phase (the XRD patterns can be indexed by Ref. [12]).

These suggest that the (Perovskite) orthorhombic and tetragonal phases coexist in the $(1-x)\text{K}_{0.5}\text{Na}_{0.5}\text{NbO}_{3-x}\text{LiSbO}_3$ ceramics with $0.045 < x < 0.055$. Similar to Ba-TiO₃, the orthorhombic phase of the ceramics demonstrates a nonprimitive cell, while the tetragonal phase is primitive. It is also noted that the diffraction peaks shift slightly towards high diffraction angles as x increases. This may be attributed to the smaller ionic radii of Li⁺ and Sb⁵⁺ than those of $(\text{Na}_{0.5}\text{K}_{0.5})^+$ and Nb⁵⁺.

In the orthorhombic region, the lattice constants c and a have very close values, which can explain why there were only two peak splitting of (2 0 0) reflections at a 2θ of 45.5° for an orthorhombic structure, rather than three peak splitting. In the tetragonal phase, the c/a ratio for the ceramics with $x = 0.055$ and 0.06 were 1.0070 and 1.0074, respectively, which indicated that the tetragonal-

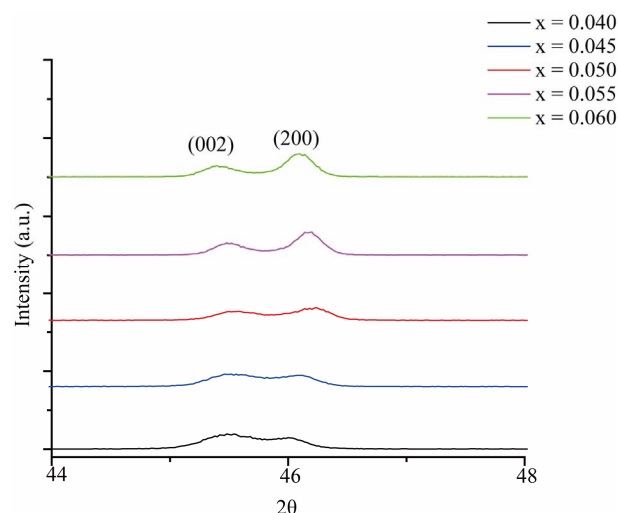


Figure 2. XRD patterns of the ceramics in the ranges of 2θ from 44° to 48° of $(1-x)\text{K}_{0.5}\text{Na}_{0.5}\text{NbO}_{3-x}\text{LiSbO}_3$ ceramics.

ity of the ceramics increased with further increasing x . In addition, it was seen that the cell volumes of the ceramics decreased gradually with the increasing x , which can explain why the diffraction peaks shifted slightly towards high diffraction angles as x increased.

3.2. SEM Analysis

The microstructure of the KNN ceramics containing x mol% of Li and Sb ($0.40 < x < 0.060$) sintered at 1060°C for 2 h was investigated using SEM. Note that instead of the fractured cross sectional SEM images, the surface morphology images have been used to elucidate the microstructure features of KNN ceramics, simply because they were confirmed to be very similar but more distinct than the fractured cross-sectional SEM images.

The KNN ceramics sintered at 1060°C had a porous microstructure with small grains, as shown in **Figure 3(a)** for $x = 0.050$ composition. However, when the sintering temperature increased to 1080°C a dense, uniform microstructure with enlarged grains was developed (**Figure 3(b)**). These enlarged grains were angular with a flat interface and the specimen showed abnormally grown

grains, as indicated by the arrow in **Figure 3(b)**. An angular grain with a flat surface is typically observed in the abnormal grain growth in the presence of the liquid phase. Therefore, it was considered that densification of the Li and Sb co-doped KNN ceramics might be explained by the liquid-phase sintering. This may be attributed to the low melting temperature of Li compounds that appears to promote the formation of a liquid phase during sintering. However, it was very difficult to find liquid phase, implying that the liquid phase formed during the sintering could be a transient liquid phase, with a high solubility in the KNN ceramics that led to its eventual disappearance with sintering time. **Figures 3(c) and 3(d)** shows the KNN ceramics sintered at 1100°C and 1120°C; enlarged grains can be observed showing an abnormal grain growth (AGG). Their relative density was found to be much less as compared to the ceramics sintered at 1080°C. It is generally agreed that AGG is caused by the existence of a liquid phase. Chun *et al.* [13] found that extensive AGG occurred on the surface of a sintered Ba-TiO₃ specimen and concluded that the BaO evaporation from the surface and consequent formation of eutectic

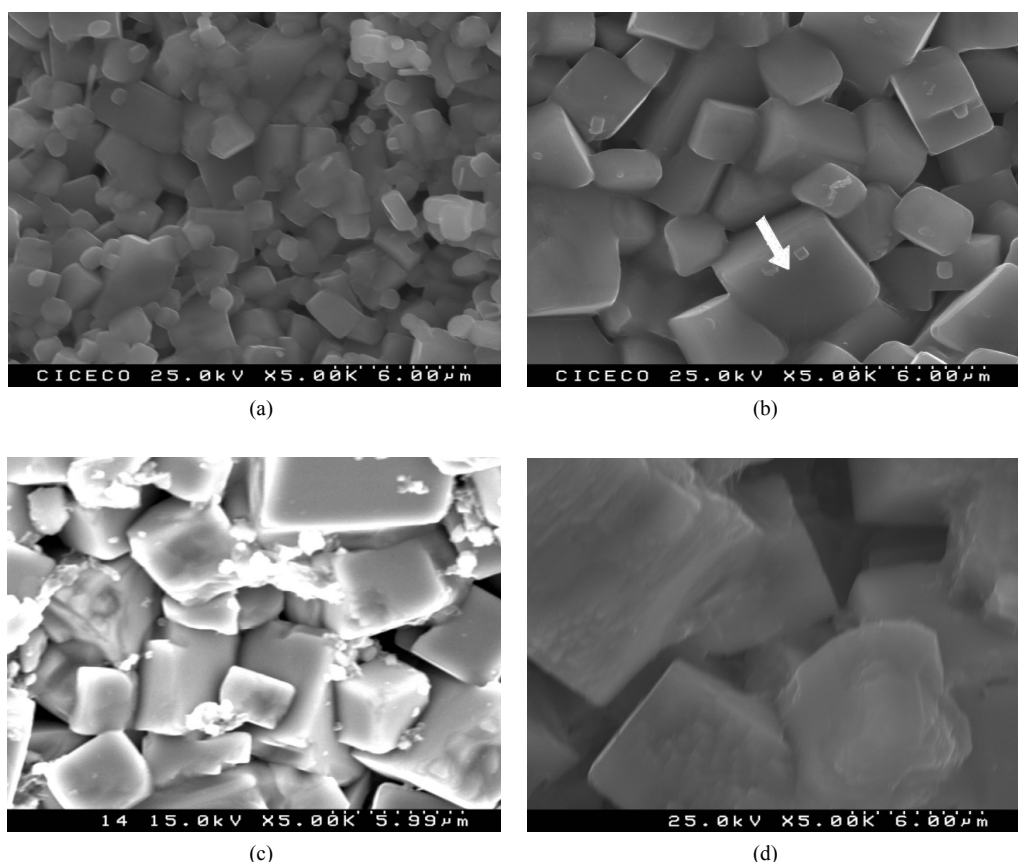


Figure 3. SEM micrographs of fractured surface of $(1 - x)K_{0.5}Na_{0.5}NbO_{3-x}LiSbO_3$ pellets ($x = 0.045$) sintered at (a) 1060°C; (b) 1080°C, (c) 1100°C and (d) 1120°C.

liquid is the cause of AGG. Thus the ceramics can be well sintered at $\sim 1080^{\circ}\text{C}$ in order to obtain a dense microstructure, which is about 200°C lower than the sintering temperature for PZT ceramics.

Although all alkali components may be volatilized during the sintering, their volatilization rates must be different at the same temperature. As a result, the final actual compositions may become different from the starting one. By referring to the report [14] for KNN ceramics with different K/Na ratios, and comparing the standard XRD patterns of KNbO₃ (#32-0822) and NaNbO₃ (#33-1270), it is likely that the Na content decreased with increasing temperature. Considering that the mass transportation for the volatilization from the interior of the sample may occur through the grain surface or grain boundary, it is reasonable to think that the compositions at some grain boundaries change toward a high K/Na ratio. According to the phase diagram of the KNbO₃-NaNbO₃ system, the solidus line temperature decreases with increasing K/Na ratio, so that the liquid phase is easy to be formed when volatilization occurs.

3.3. Density Analysis

Figure 4 shows the density of the ceramics as a function of x . After the addition of LiSbO₃, the density increases and has a high value of 4.399 g/cm^3 which is about 98.2% of the theoretical value for $x = 0.045$ at a sintering temperature of 1080°C .

Then, the bulk density gradually decreased with increasing x . The decrease in density at higher x may be attributed to the formation of the secondary phase K₃Li₂Nb₅O₁₅ of which the theoretical density is low. The densities of other ceramics were in the range of $4.023 - 4.38\text{ g/cm}^3$. These results indicated that the optimum Li and Sb addition can promote sintering and thus improve the density of ceramics. However, excess Li addition can also result in the decrease of the bulk density.

3.4. Thermal Analysis

The solid state synthesis of the KNN samples ($x = 0.045$) from alkaline carbonates and niobium oxide was followed by thermal analysis (**Figure 5**).

The sample loses 12 wt% upon heating to 700°C . A weight loss of about 1% upon heating up to 200°C accompanied by an endothermic peak is a result of H₂O removal. The presence of water content in the carbonate-oxide powder mixture is due to the hygroscopic nature of both carbonates, particularly K₂CO₃, which absorbs easily a few wt% of water in normal atmosphere where the manipulation of the precursor powder takes place. Between 380°C and 700°C there is a weight loss of 11% due to decomposition of carbonates. It occurs in two

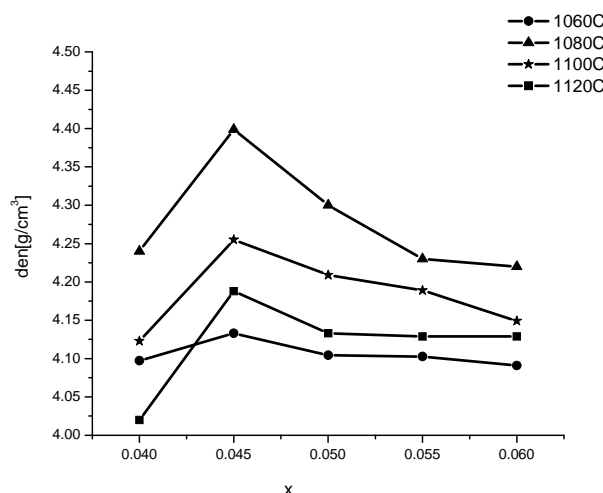


Figure 4. Density of $(1 - x)\text{K}_{0.5}\text{Na}_{0.5}\text{NbO}_{3-x}\text{LiSbO}_3$ ceramics as a function of x .

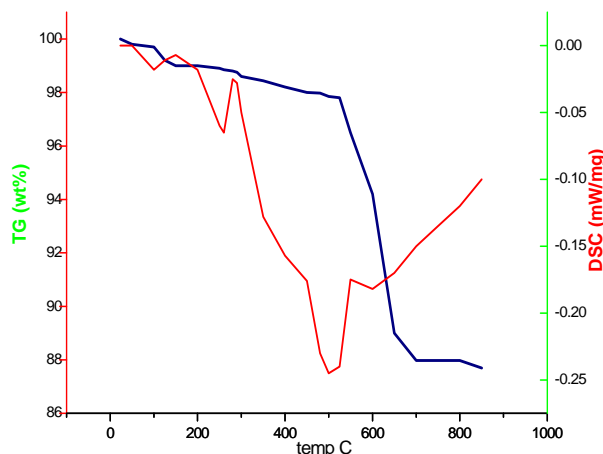


Figure 5. DSC and TGA curves of $(1 - x)\text{K}_{0.5}\text{Na}_{0.5}\text{NbO}_{3-x}\text{LiSbO}_3$ with $x = 0.045$.

steps, 5% between 380°C to 540°C and 5% between 380°C to 700°C . As both alkaline carbonates are stable at 700°C [15,16], the lowering of the decomposition temperature of the carbonates is associated with the synthesis of the alkaline niobate.

4. Conclusions

Li and Sb modified K_{0.5}Na_{0.5}NbO₃ ceramics with single perovskite phase have been synthesized by normal sintering at $1060^{\circ}\text{C} - 1120^{\circ}\text{C}$. The effects of the sintering temperature on structure and microstructure of the ceramic compounds are investigated. Using conventional solid-state processing techniques perovskite phase was achieved for all the compositions. The crystal structure changes from orthorhombic to tetragonal with increase in Li and Sb content. At a sintering temperature of 1080°C ,

a dense, uniform microstructure with enlarged grains was developed for all compositions of KNN compounds. After the addition of LiSbO₃, the density increases and was found to be maximum (98.2% of the theoretical value) for $x = 0.045$. Densification of the Li and Sb co-doped KNN ceramics might be attributed to the liquid-phase sintering present during the sintering process.

5. Acknowledgements

Authors wish to acknowledge Department of Science and Technology, Govt of India for the financial support under a research project scheme.

REFERENCES

- [1] G. H. Haerting, "Properties of Hot-Pressed Ferroelectric Alkali Niobate Ceramics," *Journal of the American Ceramic Society*, Vol. 50, No. 6, 1967, pp. 229-230.
- [2] R. E. Jaeger and L. Egerton, "Hot Pressing of Potassium-Sodium Niobates," *Journal of the American Ceramic Society*, Vol. 45, No. 5, 1962, pp. 209-213.
[doi:10.1111/j.1151-2916.1962.tb1127.x](https://doi.org/10.1111/j.1151-2916.1962.tb1127.x)
- [3] L. Egerton and D. M. Dillon, "Piezoelectric and Dielectric Properties of Ceramics in the System Potassium-Sodium Niobate," *Journal of the American Ceramic Society*, Vol. 42, No. 9, 1959, pp. 438-442.
[doi:10.1111/j.1151-2916.1959.tb12971.x](https://doi.org/10.1111/j.1151-2916.1959.tb12971.x)
- [4] M. Kosec and D. Kolar, "On Activated Sintering and Electrical Properties of NaKNbO₃," *Materials Research Bulletin*, Vol. 10, No. 5, 1975, pp. 335-340.
[doi:10.1016/0025-5408\(75\)90002-1](https://doi.org/10.1016/0025-5408(75)90002-1)
- [5] S. Narayana Murty, K. V. Ramana Murty, K. Umakantham and A. Bhanumathi, "Modified (NaK)NbO₃ Ceramics for Transducer Applications," *Ferroelectrics*, Vol. 102, No. 1, 1990, pp. 243-247.
[doi:10.1080/00150199008221484](https://doi.org/10.1080/00150199008221484)
- [6] J.-F. Li, K. Wang, B. P. Zhang and L. M. Zhang, "Ferroelectric and Piezoelectric Properties of Fine-Grained Na_{0.5}K_{0.5}NbO₃ Lead-Free Piezoelectric Ceramics Prepared by Spark Plasma Sintering," *Journal of the American Ceramic Society*, Vol. 89, No. 2, 2006, pp. 706-709.
- [7] R. P. Wang, R. J. Xie, T. Sekiya and Y. Shimojo, "Fabrication and Characterization of Potassium-Sodium Niobate Piezoelectric Ceramics by Spark-Plasma-Sintering Method," *Materials Research Bulletin*, Vol. 39, No. 11, 2004, pp. 1709-1715. [doi:10.1016/j.materresbull.2004.05.007](https://doi.org/10.1016/j.materresbull.2004.05.007)
- [8] S. Tashiro, H. Nagamatsu and K. Nagata, "Sinterability and Piezoelectric Properties of KNbO₃ Ceramics after Substituting Pb and Na for K," *Japanese Journal of Applied Physics*, Vol. 4, No. 11B, 2002, pp. 7113-7118.
[doi:10.1143/JJAP.41.7113](https://doi.org/10.1143/JJAP.41.7113)
- [9] E. Hollenstein, M. Davis, D. Damjanovic and N. Setter, "Piezoelectric Properties of Li- and Ta-Modified (Na_{0.5}K_{0.5})NbO₃ Ceramics," *Applied Physics Letters*, Vol. 87, No. 18, 2005, pp. 182905-182907.
[doi:10.1063/1.2123387](https://doi.org/10.1063/1.2123387)
- [10] M. Matsubara, T. Yamaguchi, K. Kikuta and S. Hirano, "Effect of Li Substitution on the Piezoelectric Properties of Potassium Sodium Niobate Ceramics," *Japanese Journal of Applied Physics*, Vol. 44, No. 8, 2005, pp. 6136-6142. [doi:10.1143/JJAP.44.6136](https://doi.org/10.1143/JJAP.44.6136)
- [11] International Centre for Diffraction Data, JCPDS-ICDD 2001, File No. 71-2171.
- [12] International Centre for Diffraction Data, JCPDS-ICDD 2001, File No. 71-0945.
- [13] J. S. Chun, N. M. Hwang, D. Y. Kim and J. K. Park, "Abnormal Grain Growth Occurring at the Surface of a Sintered BaTiO₃ Specimen," *Journal of the American Ceramic Society*, Vol. 87, No. 9, 2004, pp. 1779-1781.
[doi:10.1111/j.1551-2916.2004.01779.x](https://doi.org/10.1111/j.1551-2916.2004.01779.x)
- [14] B.-P. Zhang, J. F. Li and K. Wang, "Compositional Dependence of Piezoelectric Properties in Na_xK_{1-x}NbO₃ Lead-Free ceramics Prepared by Spark Plasma Sintering," *Journal of the American Ceramic Society*, Vol. 89, No. 5, 2006, pp. 1605-1609.
[doi:10.1111/j.1551-2916.2006.00960.x](https://doi.org/10.1111/j.1551-2916.2006.00960.x)
- [15] Gmelins Handbuch der Anorganischen Chemie, Verlag Chemie, Weinheim, 1969, Ch. 22, p. 834.
- [16] Gmelins Handbuch der Anorganischen Chemie, Verlag Chemie, Weinheim, 1969, Ch. 21, p. 1317.